MINISTRY OF EDUCATION AND TRAINING MINISTRY OF TRANSPORT

UNIVERSITY OF TRANSPORT TECHNOLOGY

NGUYEN VAN TIEN

NONLINEAR ELASTIC BUCKLING OF CONSTRUCTION STRUCTURES IN THE FORMS OF FG-CNTRC PLATES AND SHELLS TAKING INTO ACCOUNT STIFFENING METHODS

Major: Special Construction Engineering

Code: 9580206

SUMMARY OF DOCTORAL THESIS

HA NOI – 2024

This work is completed at: University of Transport Technology

Scientific Supervisors:

1. **Assoc.Prof.Dr. Vu Hoai Nam**
2. **Dr. Nguyen Minh Khoa**

Reviewer: Prof.Dr.Sci. Dao Huy Bich

Reviewer: Assoc.Prof.Dr. Tran The Truyen

Reviewer: Assoc.Prof.Dr. Do Van Thom

The thesis is defended before the University Council for Doctoral Thesis, meeting at the University of Transport Technology

at 8h30, date 24 month 05 year 2024

This thesis can be found at:

- National Library of Vietnam
- Library of University of Transport Technology

INTRODUCTION

1. The necessity of the thesis

Nonlinear buckling and buckling are important problems in analyzing the mechanical behavior of engineering structures in general and construction engineering in particular. The type of advanced carbon nanotube-reinforced composite material with modified mechanical properties that has received special attention in recent years is called Functionally graded carbon nanotube-reinforced composite (FG-CNTRC). Due to their superior thermo-mechanical properties, they can be widely used in engineering structures subjected to severe loads. Stiffening plate and shell structures with stiffeners is a common method. Current design standards only focus on the overall linear buckling design of isotropic plates and shells. Therefore, there is a need for theoretical research on these problems as a basis for developing structural design standards. Based on the above reasons, this thesis researches: "**Nonlinear elastic buckling of construction structures in the forms of FG-CNTRC plates and shells taking into account stiffening methods".**

2. Research objectives of the thesis

i) Propose methods to stiffen the FG-CNTRC plates and shells

ii) Develop suitable improved smeared stiffener techniques for stiffened structures

iii) Analysis of buckling and postbuckling behavior of FG-CNTRC civil structures in the forms of plates and shells with stiffeners

iv) Evaluate the effects of input parameters and other parameters of civil structures in the forms of FG-CNTRC plate and shell structures

3. Subject and scope of research of the thesis

Research object: plates and shells such as FG-CNTRC rectangular plates and cylindrical shells, considering the stiffening methods.

Research scope: nonlinear buckling and postbuckling problems.

4. Research Methodology

Theoretical research method based on analytical approach.

5. Structure of the thesis: Includes introduction, 4 chapters, conclusion, list of author's scientific works, and references.

Chapter 1. OVERVIEW OF THE RESEARCH PROBLEM

1.1. Nanocomposite materials and applications in construction

1.1.2. Functionally graded carbon nanotube reinforced composite (FG-CNTRC)

With the discovery of carbon nanotubes (CNTs) by Iijima [58, 59], CNTs have begun to receive research attention and application in many different fields of science and technology. Originating from the idea of FGM, the functionally graded (FG) distribution model of CNT was first proposed by Shen [119]. Many studies on the thermomechanical behavior of FG-CNTRC beams, plates, and shells were performed.

1.1.3. Application of Nanocomposite materials in construction

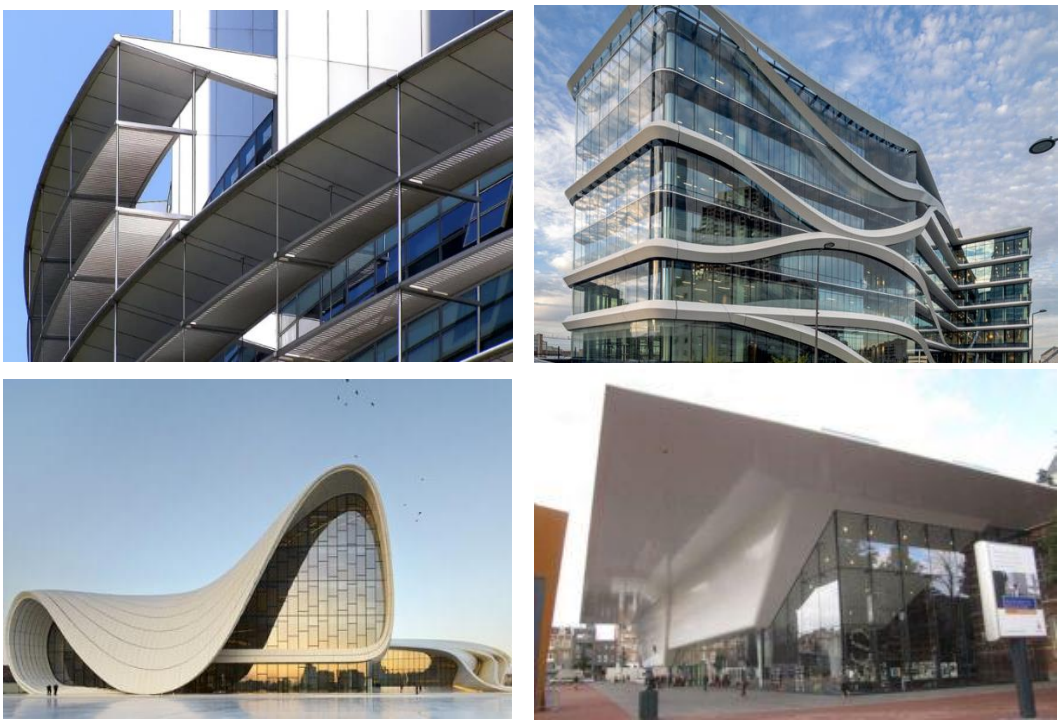

Fig. 1.1. Application of advanced composite materials for constructions [62, 94, 103, 110]

1.2. FG-CNTRC, buckling and postbuckling, and studies on thermo-mechanical behavior of FG-CNTRC structures

1.2.1. Distribution rules and mechanical properties of FG-CNTRC

According to the mixture rule, the shear modulus and effective Young's modulus can be expressed as [119-129]

$$E_{11} = \eta_1 V_{CNT} E_{11}^{CNT} + V_m E^m, \quad \frac{\eta_2}{E_{22}} = \frac{V_{CNT}}{E_{22}^{CNT}} + \frac{V_m}{E^m}, \quad \frac{\eta_3}{G_{12}} = \frac{V_{CNT}}{G_{12}^{CNT}} + \frac{V_m}{G^m}, \quad (1.1)$$

The thermal expansion coefficients in the CNT direction and the orthogonal direction can be expressed as [119-129]

$$\begin{aligned}\alpha_{11} &= V_{CNT}\alpha_{11}^{CNT} + V_m\alpha^m,\\ \alpha_{22} &= \left(1+\nu_{12}^{CNT}\right)V_{CNT}\alpha_{22}^{CNT} + \left(1+\nu^m\right)V_m\alpha^m - \nu_{12}\alpha_{11},\end{aligned} \tag{1.5}$$

Poisson ratio is determined as follows [119-129]

$$\nu_{12} = V_{CNT}^{*}\nu_{12}^{CNT} + V_m\nu^m, \tag{1.6}$$

The matrix material chosen is Poly (methyl methacrylate) (PMMA). Temperature-dependent properties are assumed to be $\nu^m = 0.34$, $\alpha^m = 45\left(1+0.0005\Delta T\right)\times 10^{-6}/\mathrm{K}$, and $E^m = \left(3.52 - 0.0034T\right) GPa$.

1.2.3. Studies on the thermomechanical behavior of FGM and FG-CNTRC plates and shells

1.2.3.1. FGM plate and shell structures

Many international authors researched FGM plates and shells such as Shen and Wang [125], Chen et al. [20], Huang and Han [53-55], Sofiyev and Schnack [131], and Vietnamese authors [7, 13, 28, 29, 89, 142, 145].

1.2.3.2. Stiffened FGM plate and shell structures

Dao Huy Bich et al. [11], Najafizadeh et al. [98].

1.2.2.3. FG-CNTRC plate and shell structures

International authors analyzed FG-CNTRC plate and shell structures such as Shen et al. [119-124, 126-129, 149], Kiani et al. [61, 63, 64, 65, 66, 67, 95, 96, Lei et al. [74, 75, 76], Liew et al. [87], Sofiyev et al. [133-135], and Vietnamese authors [25, 30-41, 8, 92, 51, 52, 143, 144…].

1.2.3.4. Auxetic structures

Typical research works on Auxetic structures are: Zhu et al. [158]. Nguyen Van Quyen et al. [109]. Pham Hoang Anh et al. [9] Le Ngoc Ly et al. [92] Lan et al. [71] Li et al. [79-82]

1.3. Potential application of FG-CNTRC shell plate structures in construction structures

With the superior characteristics of FG-CNTRC compared to traditional metal and composite materials, there is great potential for application in many construction components and especially special projects with particular requirements in bearing capacity, durability, and reliability.

Some potential applications can be seen such as water transport pipes, high-pressure compressed air transport, and cylindrical structures in marine constructions, and other special construction structures...

1.4. Domestic and international achieved results and further research requirements

1.4.1. Domestic and international achieved results

1) Linear and nonlinear static buckling problems of FG-CNTRC plate and shell structures were investigated relative-comprehensively.

2) Linear and nonlinear dynamic buckling and vibration problems of FG-CNTRC structures were also investigated relative-comprehensively.

3) The lack of research on the stiffened plate and shell structures with stiffeners can be observed.

4) Studies on the FG-CNTRC plates and shells with Auxetic core were not mentioned much.

1.4.2. Further research requirements

1) Improved smeared stiffener techniques for FG-CNTRC stiffeners need to be developed.

2) Research on nonlinear buckling and postbuckling of FG-CNTRC plates with FG-CNTRC stiffeners in thermal environment.

3) Research on buckling and postbuckling of the FG-CNTRC cylindrical shells with stiffeners subjected to different types of loads.

4) Research on nonlinear buckling and postbuckling of FG-CNTRC cylindrical shells with Auxetic core.

Chapter 2. NONLINEAR BUCKLING OF FG-CNTRC CYLINDRICAL SHELLS STIFFENED BY FG-CNTRC STIFFENERS SUBJECT TO EXTERNAL PRESSURE OR AXIAL COMPRESSION IN THERMAL ENVIRONMENT

This chapter proposes a stiffener design option made of FG-CNTRC for the FG-CNTRC cylindrical shells. The improved smeared stiffener technique for FG-CNTRC stiffeners is developed based on anisotropic beam theory combined with Lekhniskii's classical smeared stiffener technique idea. The governing equations are established based on Donnell shell theory, including von Kármán geometric nonlinearity and Pasternak

elastic foundation model. The Galerkin method is applied to obtain a system of equilibrium equations in nonlinear algebraic form.

2.1. The FG-CNTRC cylindrical shells with FG-CNTRC stiffeners and the governing equations

FG-CNTRC cylindrical shells in this thesis are studied with a coordinate system $Oxyz$ place on the middle surface of the shells as shown in Fig. 2.1. The shell is subjected to external pressure q uniformly distributed on the shell surface or axial compression p uniformly distributed on the edges and surrounded by two-parameter Pasternak elastic foundation.

In addition, the FG-CNTRC cylindrical shells are stiffened by FG-CNTRC stiffeners in the circular or longitudinal directions on the inner surface of the shell.

Expressions for extension forces N_x, N_y, N_{xy} and moments M_x, M_y, M_{xy} of stiffened FG-CNTRC cylindrical shells can be obtained by summing the stiffnesses of the stiffened shell, which are expressed as

$$\begin{bmatrix} N_x \\ N_y \\ N_{xy} \\ M_x \\ M_y \\ M_{xy} \end{bmatrix} = \begin{bmatrix} A_{11} & A_{12} & 0 & B_{11} & B_{12} & 0 \\ A_{12} & A_{22} & 0 & B_{12} & B_{22} & 0 \\ 0 & 0 & A_{66} & 0 & 0 & B_{66} \\ B_{11} & B_{12} & 0 & D_{11} & D_{12} & 0 \\ B_{12} & B_{22} & 0 & D_{12} & D_{22} & 0 \\ 0 & 0 & B_{66} & 0 & 0 & D_{66} \end{bmatrix} \begin{bmatrix} \varepsilon_x^0 \\ \varepsilon_y^0 \\ \gamma_{xy}^0 \\ -\dfrac{\partial^2 w}{\partial x^2} \\ -\dfrac{\partial^2 w}{\partial y^2} \\ -2\dfrac{\partial^2 w}{\partial x \partial y} \end{bmatrix} - \begin{bmatrix} \phi_{1x}^T \\ \phi_{1y}^T \\ 0 \\ \phi_{2x}^T \\ \phi_{2y}^T \\ 0 \end{bmatrix}, \quad (2.8)$$

The stiffnesses of the shell with longitudinal stiffeners are obtained as

$$\left(A_{11}, B_{11}, D_{11}\right) = \left(A_{11}^{sh}, B_{11}^{sh}, D_{11}^{sh}\right) + \left(A_{11}^{stff-L}, B_{11}^{stff-L}, D_{11}^{stff-L}\right), \quad (2.9)$$

$$\begin{aligned} &\left(A_{22}, A_{12}, A_{66}, B_{22}, B_{12}, B_{66}, D_{22}, D_{12}, D_{66},\right) \\ &\quad = \left(A_{22}^{sh}, A_{12}^{sh}, A_{66}^{sh}, B_{22}^{sh}, B_{12}^{sh}, B_{66}^{sh}, D_{22}^{sh}, D_{12}^{sh}, D_{66}^{sh}\right), \end{aligned} \quad (2.10)$$

Stiffnesses of longitudinal stiffeners $A_{11}^{stff-L}, B_{11}^{stff-L}, D_{11}^{stff-L}$ are calculated

$$\begin{bmatrix} A_{11}^{stff-L} & B_{11}^{stff-L} \\ B_{11}^{stff-L} & D_{11}^{stff-L} \end{bmatrix} = \begin{bmatrix} \hat{A}_{11}^{L} & \hat{B}_{11}^{L} \\ \hat{B}_{11}^{L} & \hat{D}_{11}^{L} \end{bmatrix}$$

$$- \begin{bmatrix} \hat{A}_{12}^{L} & 0 & \hat{B}_{12}^{L} & 0 \\ \hat{B}_{12}^{L} & 0 & \hat{D}_{12}^{L} & 0 \end{bmatrix} \begin{bmatrix} \hat{A}_{22}^{L} & 0 & \hat{B}_{22}^{L} & 0 \\ 0 & \hat{A}_{66}^{L} & 0 & \hat{B}_{66}^{L} \\ \hat{B}_{22}^{L} & 0 & \hat{D}_{22}^{L} & 0 \\ 0 & \hat{B}_{66}^{L} & 0 & \hat{D}_{66}^{L} \end{bmatrix}^{-1} \begin{bmatrix} \hat{A}_{12}^{L} & \hat{B}_{12}^{L} \\ 0 & 0 \\ \hat{B}_{12}^{L} & \hat{D}_{12}^{L} \\ 0 & 0 \end{bmatrix}, \quad (2.14)$$

with Ω_L is the integral region over the height of the stiffeners.

Internal thermal forces of the shells with L stiffeners can be determined as follows

$$\phi_{1x} = \phi_{1x}^{sh} + \phi_{1x}^{stff}, \qquad \phi_{1y} = \phi_{1y}^{sh}, \quad (2.18)$$

and for L stiffeners are presented by

$$\phi_{1x}^{stff} = \frac{b_{stff}^{L}}{d_{stff}^{L}} \int_{\Omega_L} (Q_{11}\alpha_{11} + Q_{12}\alpha_{22})\Delta T dz, \quad (2.21)$$

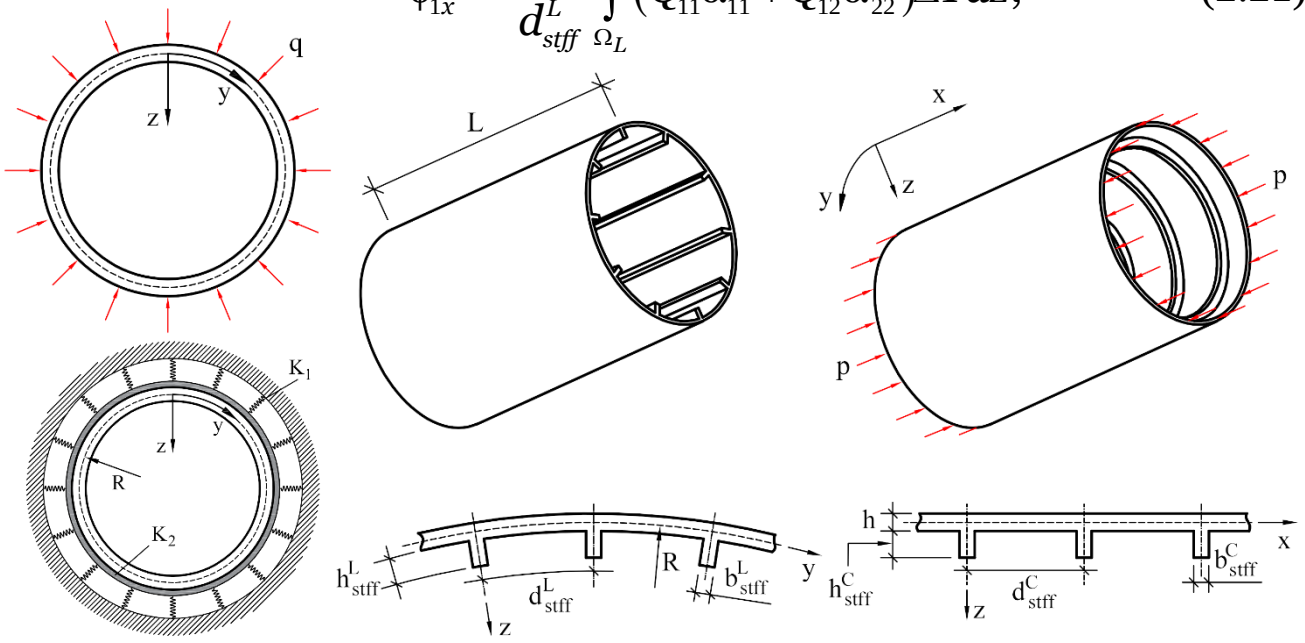

Fig. 2.1. Geometric parameters and coordinate system of FG-CNTRC cylindrical shells stiffened by FG-CNTRC stiffeners surrounded by elastic foundation

The compatibility equation can be obtained directly from Eq. (2.7), as

$$\frac{\partial^2 \varepsilon_x^0}{\partial y^2} + \frac{\partial^2 \varepsilon_y^0}{\partial x^2} - \frac{\partial^2 \gamma_{xy}^0}{\partial x \partial y} + \frac{1}{R}\frac{\partial^2 w}{\partial x^2} - \frac{\partial^2 w}{\partial x \partial y} + \frac{\partial^2 w}{\partial x^2}\frac{\partial^2 w}{\partial y^2} = 0. \quad (2.22)$$

Equilibrium equations according to nonlinear Donnell shell theory are [3]

$$\frac{\partial N_x}{\partial x}+\frac{\partial N_{xy}}{\partial y}=0,\quad \frac{\partial N_{xy}}{\partial x}+\frac{\partial N_y}{\partial y}=0,$$

$$\frac{\partial^2 M_x}{\partial x^2}+2\frac{\partial^2 M_{xy}}{\partial x\partial y}+\frac{\partial^2 M_y}{\partial y^2}+\frac{N_y}{R} \tag{2.23}$$

$$+N_x\frac{\partial^2 w}{\partial x^2}+2N_{xy}\frac{\partial^2 w}{\partial x\partial y}+N_y\frac{\partial^2 w}{\partial y^2}=-q+K_1 w-K_2\left(\frac{\partial^2 w}{\partial x^2}+\frac{\partial^2 w}{\partial y^2}\right),$$

The third equation of (2.23) can be rewritten by substituting Eqs. (2.8) and (2.24) into this equation, leading to

$$\Theta\equiv D_{11}^*\frac{\partial^4 w}{\partial x^4}+\left(D_{12}^*+D_{21}^*+4D_{66}^*\right)\frac{\partial^4 w}{\partial x^2\partial y^2}+D_{22}^*\frac{\partial^4 w}{\partial y^4}$$

$$+B_{21}^*\frac{\partial^4 \chi}{\partial x^4}-\left(B_{11}^*+B_{22}^*-2B_{66}^*\right)\frac{\partial^4 \chi}{\partial x^2\partial y^2}-B_{12}^*\frac{\partial^4 \chi}{\partial y^4}-\frac{\partial^2 \chi}{\partial y^2}\frac{\partial^2 w}{\partial x^2} \tag{2.25}$$

$$-\frac{\partial^2 \chi}{\partial x^2}\frac{\partial^2 w}{\partial y^2}+2\frac{\partial^2 \chi}{\partial x\partial y}\frac{\partial^2 w}{\partial x\partial y}-\frac{1}{R}\frac{\partial^2 \chi}{\partial x^2}-q+K_1 w-K_2\left(\frac{\partial^2 w}{\partial x^2}+\frac{\partial^2 w}{\partial y^2}\right)=0.$$

The deformation compatibility equation (2.22), combined with equations (2.8) and (2.24) becomes

$$A_{11}^*\frac{\partial^4 \chi}{\partial x^4}+\left(A_{66}^*-2A_{12}^*\right)\frac{\partial^4 \chi}{\partial x^2\partial y^2}+A_{22}^*\frac{\partial^4 \chi}{\partial y^4}+B_{21}^*\frac{\partial^4 w}{\partial x^4}+B_{12}^*\frac{\partial^4 w}{\partial y^4}$$

$$+\left(B_{11}^*+B_{22}^*-2B_{66}^*\right)\frac{\partial^4 w}{\partial x^2\partial y^2}-\left(\frac{\partial^2 w}{\partial x\partial y}\right)^2+\frac{\partial^2 w}{\partial x^2}\frac{\partial^2 w}{\partial y^2}+\frac{1}{R}\frac{\partial^2 w}{\partial x^2}=0, \tag{2.26}$$

2.2. Boundary conditions and solution methods

The deflection of the shell satisfies the boundary condition (2.27) in an approximate sense chosen in the form of three terms as follows [53, 54]

$$w=\kappa_0+\kappa_1\sin\frac{m\pi x}{L}\sin\frac{ny}{R}+\kappa_2\sin^2\frac{m\pi x}{L}, \tag{2.28}$$

Substituting expression (2.28) into Eq. (2.26), the stress function form is determined by

$$\chi=Q_1\cos\frac{2m\pi x}{L}+Q_2\cos\frac{2ny}{R}$$

$$-Q_3\sin\frac{m\pi x}{L}\sin\frac{ny}{R}+Q_4\sin\frac{3m\pi x}{L}\sin\frac{ny}{R}-\frac{\sigma_{0y}hx^2}{2}-\frac{phy^2}{2}, \tag{2.29}$$

Substituting the expressions (2.28) and (2.29) into Eq. (2.25). The Galerkin method is then applied to the three deflection terms, leading to

$$\frac{\sigma_{0y}h}{R}=q-\frac{K_1\left(\kappa_2+2\kappa_0\right)}{2}, \tag{2.31}$$

$$\left(D+\frac{B^2}{A}\right)f_1+\left(\frac{m^4\pi^4}{16A_{22}^*}+\frac{n^4L^4}{16A_{11}^*R^4}\right)\kappa_1^3+m^4n^4\pi^4\left(\frac{L}{R}\right)^4\left(\frac{1}{A}+\frac{1}{E}\right)\kappa_1\kappa_2^2$$
$$+\left[\frac{2Bm^2n^2\pi^2L^2}{AR^2}-\frac{n^2L^2\left(L^2/R-4B_{21}^*m^2\pi^2\right)}{4A_{11}^*R^2}\right]\kappa_1\kappa_2-\frac{\sigma_{0y}hn^2L^4}{R^2}\kappa_1 \tag{2.32}$$
$$-m^2\pi^2L^2hp\kappa_1+L^4K_1\kappa_1+L^2K_2\kappa_1\left[\left(\frac{Ln}{R}\right)^2+\left(m\pi\right)^2\right]=0,$$

$$\left\{\left[4B_{21}^*\left(\frac{m\pi}{L}\right)^4-\frac{1}{R}\left(\frac{m\pi}{L}\right)^2\right]\frac{n^2L^2}{16A_{11}^*m^2\pi^2R^2}+\frac{B}{2A}\left(\frac{m\pi}{L}\right)^2\left(\frac{n}{R}\right)^2\right\}\kappa_1^2$$
$$+\left\{4D_{11}^*\left(\frac{m\pi}{L}\right)^4-\left[4B_{21}^*\left(\frac{m\pi}{L}\right)^4-\frac{1}{R}\left(\frac{m\pi}{L}\right)^2\right]\frac{L^2/R-4B_{21}^*m^2\pi^2}{4A_{11}^*m^2\pi^2}\right\}\kappa_2 \tag{2.33}$$
$$+\frac{1}{2}m^2n^2\pi^2\left(\frac{\pi mn}{R^2}\right)^2\left(\frac{1}{A}-\frac{1}{E}\right)\kappa_1^2\kappa_2$$
$$+\frac{\sigma_{0y}h}{R}-q-ph\left(\frac{m\pi}{L}\right)^2\kappa_2+K_1\left(\kappa_2\frac{3}{4}+\kappa_0\right)+K_2\kappa_2\left(\frac{m\pi}{L}\right)^2=0.$$

The closed condition is added in the average sense [53-55]

$$\int_0^{2\pi R}\int_0^L\frac{\partial v}{\partial y}dxdy=0. \tag{2.34}$$

2.2.1. Nonlinear buckling analysis of FG-CNTRC cylindrical shells with FG-CNTRC stiffeners subjected to external pressure $(p=0)$

Substituting σ_{0y} in expression (2.31) into Eqs. (2.32), (2.33), and (2.35), and applying $p=0$, the new forms of the equilibrium equations is

$$\kappa_0=\frac{J_{32}}{2J_{31}}\kappa_1^2-\frac{1}{2}\kappa_2-\frac{J_{34}}{2J_{31}}+\frac{J_{33}}{2J_{31}}q, \tag{2.36}$$

$$J_{11}+J_{12}\kappa_0+J_{13}\kappa_1^2+J_{14}\kappa_2+J_{15}\kappa_2^2-J_{16}q=0, \tag{2.37}$$

$$\kappa_1^2 = \frac{-J_{23}\kappa_2}{J_{21} + J_{22}\kappa_2}, \tag{2.38}$$

Substituting κ_0, κ_1^2 from Eqs. (2.36) and (2.38) into Eq. (2.37), as

$$q = \left\{ J_{11} - \frac{J_{12}J_{34}}{2J_{31}} - \left[\frac{J_{12}J_{23}J_{32}}{2J_{31}\left(J_{21} + J_{22}\kappa_2\right)} + \left(J_{14} - \frac{J_{12}}{2} \right) \right] \kappa_2 - \right.$$
$$\left. + J_{15}\kappa_2^2 - J_{13}\frac{J_{23}\kappa_2}{J_{21} + J_{22}\kappa_2} \right\} \frac{2J_{31}}{2J_{31}J_{16} - J_{12}J_{33}}. \tag{2.39}$$

The maximum deflection is obtained as

$$W_{\max} = q\frac{J_{33}}{2J_{31}} - \frac{J_{34}}{2J_{31}} - \frac{J_{32}J_{23}\kappa_2}{2J_{31}\left(J_{21} + J_{22}\kappa_2\right)} + \frac{\kappa_2}{2} + \left(\frac{-J_{23}\kappa_2}{J_{21} + J_{22}\kappa_2} \right)^{1/2}. \tag{2.42}$$

2.2.2. Nonlinear buckling analysis of FG-CNTRC cylindrical shells with FG-CNTRC stiffeners subjected to axial compression $(q = 0)$

Substitute the average stress in the σ_{0y} inner ring direction (2.31) into equations (2.32), (2.33) and (2.35), and let $q = 0$, get

$$\kappa_0 = \frac{J_{32}}{2J_{31}}\kappa_1^2 - \frac{J_{35}}{2J_{31}}p - \frac{1}{2}\kappa_2 - \frac{J_{34}}{2J_{31}}, \tag{2.43}$$

$$J_{11} + J_{12}\kappa_0 + J_{13}\kappa_1^2 + J_{14}\kappa_2 + J_{15}\kappa_2^2 - J_{17}p = 0, \tag{2.44}$$

$$\kappa_1^2 = \frac{J_{24}\kappa_2 p - J_{23}\kappa_2}{J_{21} + J_{22}\kappa_2}, \tag{2.45}$$

Substituting κ_0 and κ_1^2 from equations (2.43) and (2.45) into Eq. (2.44), the relation of p and κ_2 can be determined as follows

$$p = \left(J_{11} + J_{14}\kappa_2 - J_{12}\frac{1}{2}\kappa_2 - J_{12}\frac{J_{34}}{2J_{13}} + J_{15}\kappa_2^2 - J_{12}\frac{J_{32}}{2J_{31}}\frac{J_{23}\kappa_2}{J_{21} + J_{22}\kappa_2} - \right.$$
$$\left. \frac{J_{13}J_{23}\kappa_2}{J_{21} + J_{22}\kappa_2} \right) \left(-J_{12}\frac{J_{32}}{2J_{31}}\frac{J_{24}\kappa_2}{J_{21} + J_{22}\kappa_2} - \frac{J_{13}J_{24}\kappa_2}{J_{21} + J_{22}\kappa_2} + J_{17} + J_{12}\frac{J_{35}}{2J_{31}} \right)^{-1}. \tag{2.46}$$

Substituting equations (2.43) and (2.45) into expression (2.41), the maximum deflection of the shell can be rewritten as

$$\mathrm{W}_{\max} = \frac{J_{32}}{2J_{31}}\frac{J_{24}\kappa_2 p - J_{23}\kappa_2}{J_{21} + J_{22}\kappa_2} - \frac{J_{35}p}{2J_{31}} + \frac{\kappa_2}{2} - \frac{J_{34}}{2J_{31}} + \sqrt{\frac{J_{24}\kappa_2 p - J_{23}\kappa_2}{J_{21} + J_{22}\kappa_2}}. \tag{2.48}$$

The shortening $\bar{\Delta}_x$ is determined as

$$\bar{\Delta}_x = A_{22}^* ph + \frac{A_{12}^* RK_1\kappa_2}{2} + A_{12}^* RK_1\left(\frac{J_{32}}{2J_{31}}\frac{J_{24}\kappa_2 p - J_{23}\kappa_2}{J_{21}+J_{22}\kappa_2} - \frac{J_{35}p}{2J_{31}} - \frac{\kappa_2}{2} - \frac{J_{34}}{2J_{31}}\right) + \frac{\kappa_2^2}{4}\left(\frac{m\pi}{L}\right)^2 + \frac{1}{8}\left(\frac{m\pi}{L}\right)^2 \frac{J_{24}\kappa_2 p - J_{23}\kappa_2}{J_{21}+J_{22}\psi_2} - \left(A_{22}^*\phi_{1x}^T - A_{12}^*\phi_{1y}^T\right). \quad (2.50)$$

2.4. Applying theoretical results to nonlinear buckling analysis of FG-CNTRC cylindrical shells with FG-CNTRC stiffeners subjected to external pressure

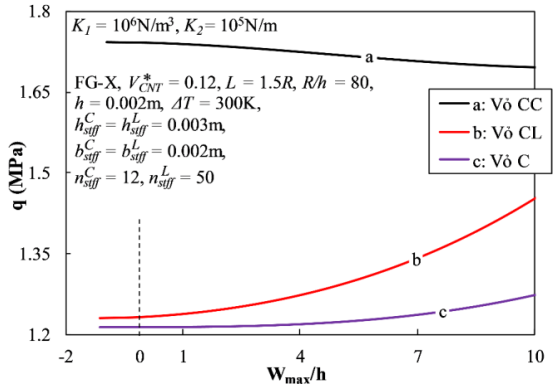

Fig. 2.5. Effect of rib direction on postbuckling curve of C-FG-CNTRC cylindrical shell

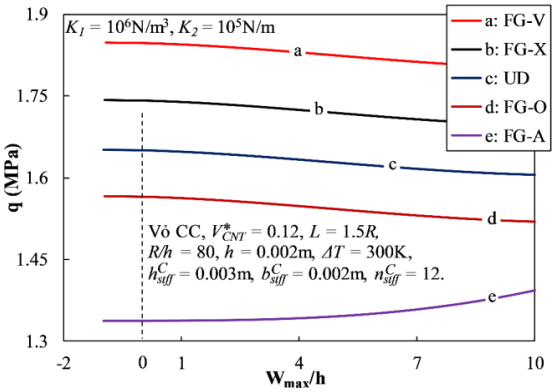

Fig. 2.9. Effect of the CNT distribution law on the postbuckling curve of the C-FG-CNTRC cylindrical shell

2.5. Applying theoretical results to nonlinear buckling analysis of FG-CNTRC cylindrical shells with FG-CNTRC stiffeners subjected to axial compression

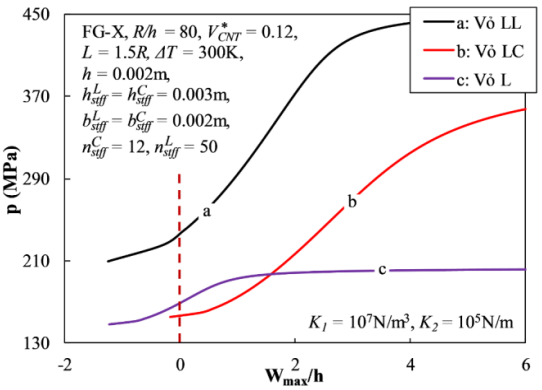

Fig. 2.12. Effect of FG-CNTRC stiffener direction on postbuckling curve $p - W_{\max}/h$ of the L-FG-CNTRC shell

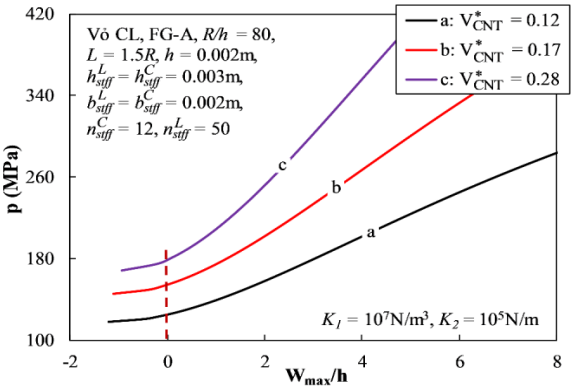

Fig. 2.22. Effect of CNT volume fraction on postbuckling curve $p - W_{\max}/h$ of the C-FG-CNTRC shell

2.6. Conclusion of Chapter 2

From the numerical results, the outstanding remarks are obtained

1. FG-CNTRC stiffeners largely affect the critical buckling pressure and postbuckling load-carrying capacity of the shells. The maximum critical buckling pressure is achieved with the FG-V CC shells.

2. The snap-through phenomenon was not observed for the L-FG-CNTRC cylindrical shell in all numerical investigations.

3. Geometric parameters, thermal environment, elastic foundation, and CNT volume fraction largely affect the buckling behavior of the shell.

4. FG-CNTRC stiffeners largely improve the critical axial compression and postbuckling capacity of the FG-CNTRC cylindrical shells.

5. The designs of CNT distribution rules of the shell and stiffeners largely affect to the effect of the FG-CNTRC stiffeners.

6. Pasternak elastic foundation, geometrical parameters, material, and thermal environment largely affect the buckling behavior of the shell.

Chapter 3. NONLINEAR BUCKLING OF FG-CNTRC CYLINDRICAL SHELLS UNDER TORSION AND STIFFENED BY FG-CNTRC STIFFENERS OR AUXETIC CORE

The FG-CNTRC cylindrical shells are considered in a more complex load case, that is torsion load, with two cases of the FG-CNTRC cylindrical shells with stiffeners and with Auxetic core.

3.1. Material and structural designs

3.1.1. Design of FG-CNTRC cylindrical shells with FG-CNTRC stiffeners

The FG-CNTRC cylindrical shells with stiffeners, the distribution rules of CNTs, and the coordinate system are similar to Chapter 2.

3.1.2. Design of sandwich FG-CNTRC cylindrical shells with Auxetic core

An FG-CNTRC sandwich cylindrical shell with an Auxetic core subjected to uniformly distributed torsion τ is considered. The geometrical parameters of the cylindrical shell, honeycomb Auxetic core, and FG-CNTRC coating layers are shown in Fig. 3.1.

Instead of calculating with a complex honeycomb core structure, we can analyze the behavior of the core layer as an anisotropic homogeneous layer with elastic constants estimated as follows [150]

$$E_{11}^{Aux} = E^m \frac{\theta_2^3\left(\theta_1 - \sin\gamma\right)}{\cos^3\gamma\left[1+\left(\tan^2\gamma + \theta_1\sec^2\gamma\right)\theta_2^2\right]}, \tag{3.7}$$

$$E_{22}^{Aux} = E^m \frac{\theta_2^3}{\cos\gamma\left(\theta_1 - \sin\gamma\right)\left(\tan^2\gamma + \theta_2^2\right)}, \tag{3.8}$$

$$G_{12}^{Aux} = E^m \frac{\theta_2^3}{\theta_1\left(1+2\theta_1\right)\cos\gamma}, \tag{3.9}$$

$$\nu_{12}^{Aux} = -\frac{\sin\gamma\left(1-\theta_2^2\right)\left(\theta_1 - \sin\gamma\right)}{\left[1+\left(\theta_1\sec^2\gamma + \tan^2\gamma\right)\theta_2^2\right]\cos^2\gamma}, \tag{3.10}$$

$$\nu_{21}^{Aux} = -\frac{\sin\gamma\left(1-\theta_2^2\right)}{\left(\tan^2\gamma + \theta_2^2\right)\left(\theta_1 - \sin\gamma\right)}, \tag{3.11}$$

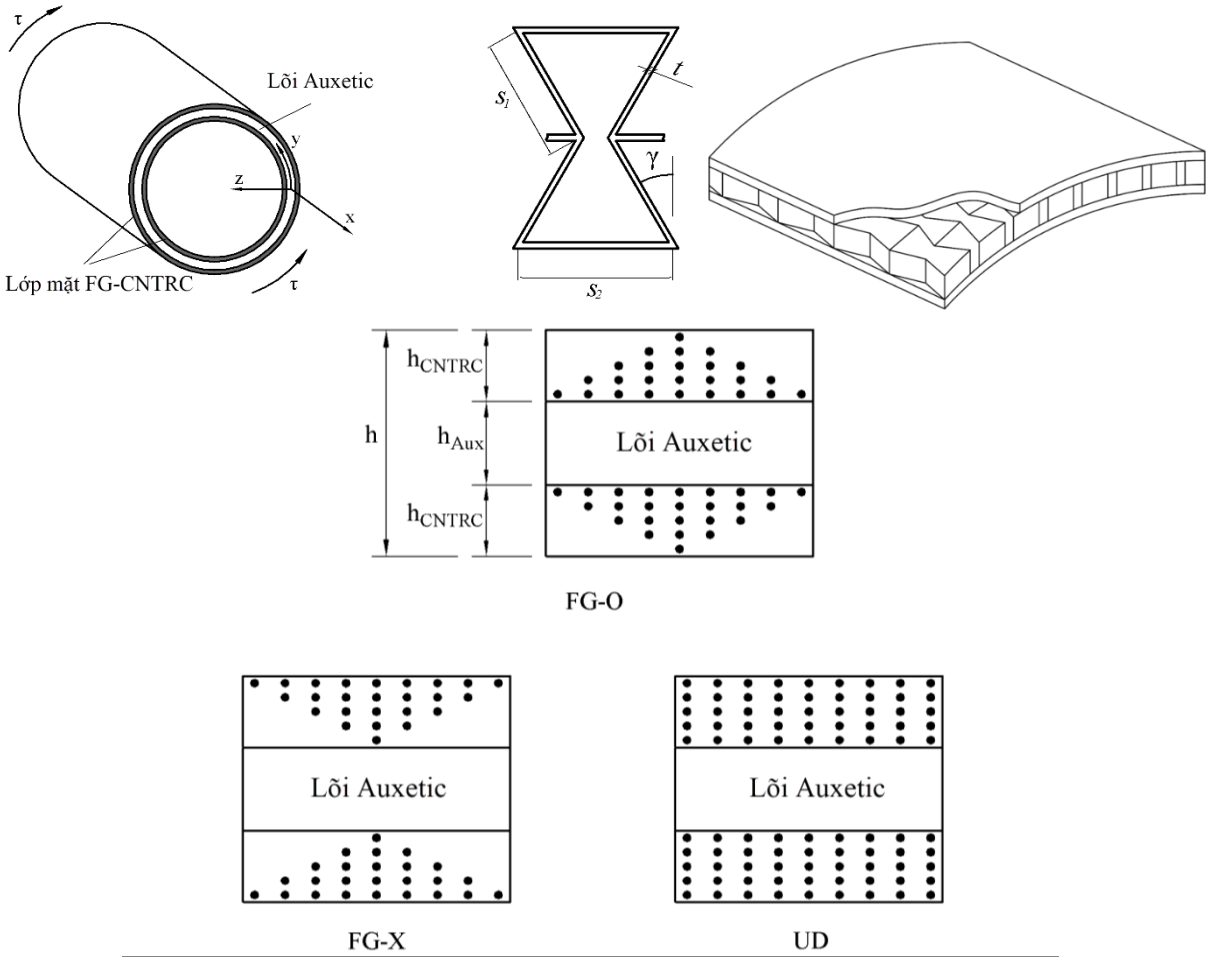

Fig. 3.1. Design of the FG-CNTRC cylindrical shell with Auxetic core

3.2. Nonlinear equilibrium equation system and stress function

The expressions of the stiffness matrix components and internal thermal forces are determined as

$$\left(A_{ij},B_{ij},D_{ij}\right)=\left(A_{ij}^{CNTRC},B_{ij}^{CNTRC},D_{ij}^{CNTRC}\right)+\left(A_{ij}^{Aux},B_{ij}^{Aux},D_{ij}^{Aux}\right), \quad (3.12)$$

$$\phi_{1x}^{T}=\phi_{1y}^{T}=0, \qquad \phi_{2x}^{T}=\phi_{2y}^{T}=0, \quad (3.13)$$

where

$$\left(A_{ij}^{CNTRC},B_{ij}^{CNTRC},D_{ij}^{CNTRC}\right)= \int_{\Pi_{out}} Q_{ij}^{CNTRC-out}\left(1,z,z^2\right)dz+\int_{\Pi_{inn}} Q_{ij}^{CNTRC-inn}\left(1,z,z^2\right)dz,\ \left(i,j=1,2,6\right) \quad (3.14)$$

$$\left(A_{ij}^{Aux},B_{ij}^{Aux},D_{ij}^{Aux}\right)=\int_{\Pi_{Aux}} Q_{ij}^{Aux}\left(1,z,z^2\right)dz, \quad \left(i,j=1,2,6\right) \quad (3.15)$$

with Π_{out} and Π_{inn} is the thickness region of the outside and inside CNTRC layers, Π_{Aux} is the thickness region of the Auxetic core.

The equilibrium equations of the cylindrical shell according to Donnell shell theory and von-Karman geometric nonlinearity, is presented as

$$\frac{\partial N_x}{\partial x}+\frac{\partial N_{xy}}{\partial y}=0, \quad (3.16)$$

$$\frac{\partial N_{xy}}{\partial x}+\frac{\partial N_y}{\partial y}=0, \quad (3.17)$$

$$\frac{\partial^2 M_x}{\partial x^2}+2\frac{\partial^2 M_{xy}}{\partial x\partial y}+\frac{\partial^2 M_y}{\partial y^2}+\frac{N_y}{R}+N_x\frac{\partial^2 w}{\partial x^2}+2N_{xy}\frac{\partial^2 w}{\partial x\partial y}+N_y\frac{\partial^2 w}{\partial y^2}=0, \quad (3.18)$$

3.3. Deflection form and Galerkin method

The three-term solution form of the deflection can be chosen as follows [55]

$$w=w(x,y)=\vartheta_0+\vartheta_1\sin\alpha x\sin\beta\left(y-\lambda x\right)+\vartheta_2\sin^2\alpha x, \quad (3.22)$$

The expression for the stress function can be determined by substituting the deflection form in equation (3.22) into equation (3.20), after some calculations to obtain

$$\begin{aligned}\chi=&F_1\cos2\alpha x+F_2\cos2\beta\left(y-\lambda x\right)\\&+F_3\cos\beta\left[y+\left(\frac{\alpha}{\beta}-\lambda\right)x\right]+F_4\cos\beta\left[y-\left(\frac{\alpha}{\beta}+\lambda\right)x\right]\\&+F_5\cos\beta\left[y-\left(\frac{3\alpha}{\beta}+\lambda\right)x\right]+F_6\cos\beta\left[y+\left(\frac{3\alpha}{\beta}-\lambda\right)x\right]-\tau hxy,\end{aligned} \quad (3.23)$$

Substituting equations (3.22) and (3.23) into the equilibrium equation (3.19), then applying the Galerkin method, the new system of balance equations in algebraic form is obtained as follows

$$2\tau h\beta^2\lambda + N_1 + N_2\vartheta_2 + N_3\vartheta_1^2 + N_4\vartheta_2^2 = 0, \tag{3.24}$$

$$N_5\vartheta_2 - N_6\vartheta_1^2 + N_7\vartheta_1^2\vartheta_2 = 0, \tag{3.25}$$

Circular shell structures rotate tightly like cylindrical shells subject to torsion and must also satisfy the closed perimeter condition below [55]

$$\int_0^{2\pi R}\int_0^{L}\frac{\partial v}{\partial y}dxdy = 0. \tag{3.26}$$

Substituting the relations (2.7), (2.8), and (2.24), taking into account (3.22), into equation (3.26), we have

$$2\vartheta_0 + \vartheta_2 + 2R\left(A_{11}^{*}\phi_{1y}^{T} - A_{12}^{*}\phi_{1x}^{T}\right) - \frac{1}{4}R\vartheta_1^2\beta^2 = 0. \tag{3.27}$$

Eliminating ϑ_0 and ϑ_2 from Eqs. (3.24), (3.25), and (3.27) and solving τ accordingly ϑ_1, contact expression τ-ϑ_1 receive the following

$$\tau = -\frac{1}{2h\beta^2\lambda}\left\{\frac{2N_2N_6\vartheta_1^2}{2\left(N_5 + N_7\vartheta_1^2\right)} + N_1 + N_3\vartheta_1^2 + N_4\left[\frac{2N_6\vartheta_1^2}{2\left(N_5 + N_7\vartheta_1^2\right)}\right]^2\right\}. \tag{3.28}$$

When $\vartheta_1 \to 0$, equation (3.28) leads to

$$\tau^{upper} = -\frac{N_1}{2h\beta^2\lambda}. \tag{3.29}$$

The dimensionless maximum deflection is rewritten in terms of the linear deflection amplitude of the postbuckling state, resulting

$$\bar{W} = W_{\max}/h = \frac{R\vartheta_1^2\beta^2}{8h} - \frac{R\left(A_{11}^{*}\phi_{1y}^{T} - A_{12}^{*}\phi_{1x}^{T}\right)}{h} + \frac{\vartheta_1}{h} + \frac{2N_6\vartheta_1^2}{4h\left(N_5 + N_7\vartheta_1^2\right)}. \tag{3.30}$$

The torsion angle is defined in the average sense as follows [55]

$$\varphi = \frac{1}{2\pi RL}\int_0^{2\pi R}\int_0^{L}\left(\frac{\partial u}{\partial y} + \frac{\partial v}{\partial x}\right)dxdy = A_{66}^{*}\tau h + \frac{n^2\lambda\vartheta_1^2}{4R^2}. \tag{3.31}$$

3.5. Applying theoretical results to nonlinear buckling analysis of FG-CNTRC cylindrical shells FG-CNTRC stiffeners subjected to torsion

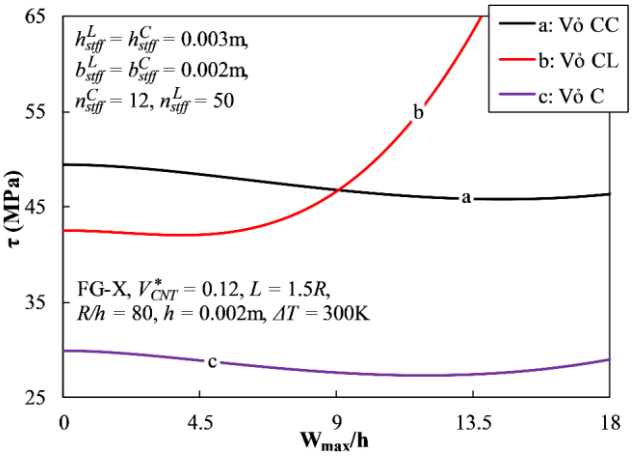

Fig. 3.6. Effect of stiffener direction on torsional postbuckling curve $\tau - \bar{W}$ of C-FG-CNTRC cylindrical shells

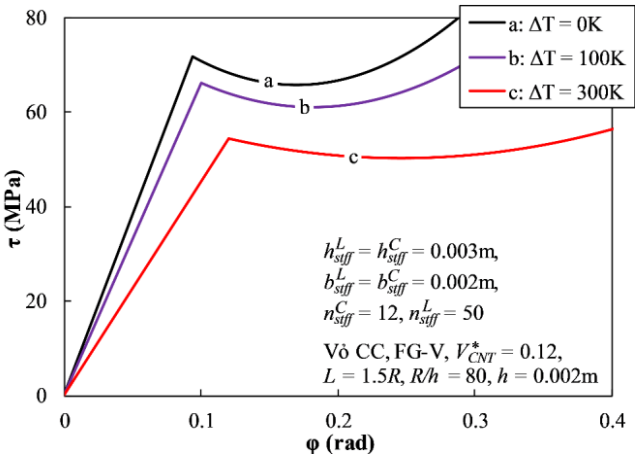

Fig. 3.14. Effect of thermal temperature on torsional postbuckling curve $\tau - \varphi$ of FG-CNTRC cylindrical shells

3.6. Applying theoretical results to nonlinear buckling analysis of FG-CNTRC cylindrical shells with Auxetic core subjected to torsion

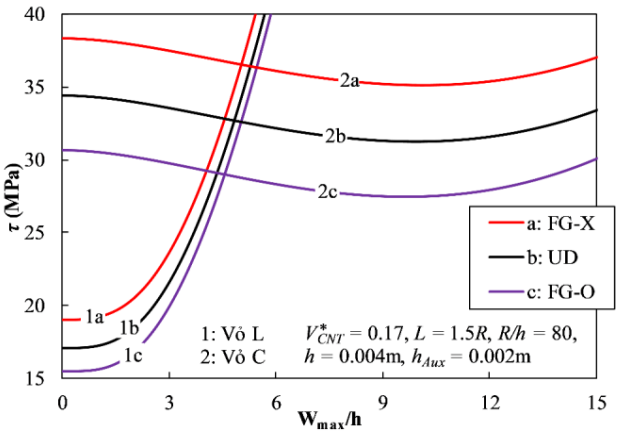

Fig. 3.17. Torsional postbuckling curves $\tau - \bar{W}$ with three CNT distribution rules of sandwich cylindrical shell with Auxetic core

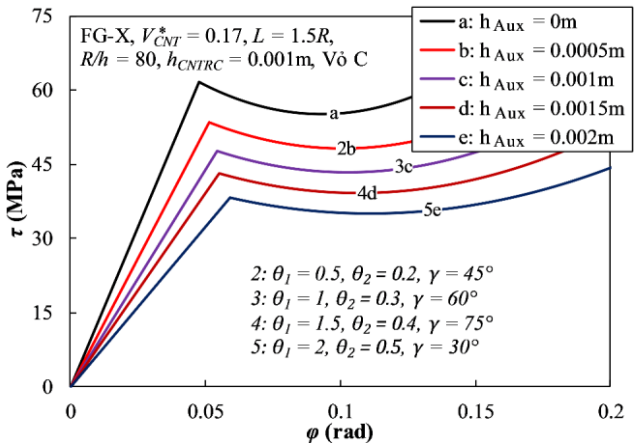

Fig. 3.26. Torsional postbuckling curves τ-φ with different geometrical parameters of cylindrical shell with Auxetic core

3.7. Conclusion of Chapter 3

For FG-CNTRC cylindrical shell with stiffeners subjected to torsion

1. The torsion load capacity of the FG-CNTRC shells with FG-CNTRC stiffeners is much greater than that of corresponding unstiffened shells.

2. The greatest effect of stiffeners is obtained for circumferential stiffeners.

3. The angle of the pre-buckling straight line $\tau - \varphi$ remains unchanged in cases with and without stiffeners.

For sandwich FG-CNTRC cylindrical shells with Auxetic core

1. The critical buckling torsion of the L-FG-CNTRC cylindrical shell is much smaller than that of the C-FG-CNTRC cylindrical shell

2. The influence of the geometric properties of the Auxetic core on the critical torsional buckling load of the shell is insignificant.

3. The thickness of the Auxetic core strongly influences the critical buckling torsion and the postbuckling load-carrying capacity of the shells.

Chapter 4. NONLINEAR BUCKLING OF FG-CNTRC PLATES STIFFENED BY FG-CNTRC STIFFENERS UNDER COMBINED LOADS ACCORDING TO HIGHER-ORDER SHEAR DEFORMATION THEORY

4.1. The design of the FG-CNTRC plates stiffened by the FG-CNTRC stiffeners

Consider the FG-CNTRC rectangular plates stiffened by FG-CNTRC stiffeners, subjected to axial compression P_x and external pressure q in thermal environment. Where, CNT is reinforced into the isotropic matrix in the longitudinal or transverse directions of the plates (Fig. 4.1).

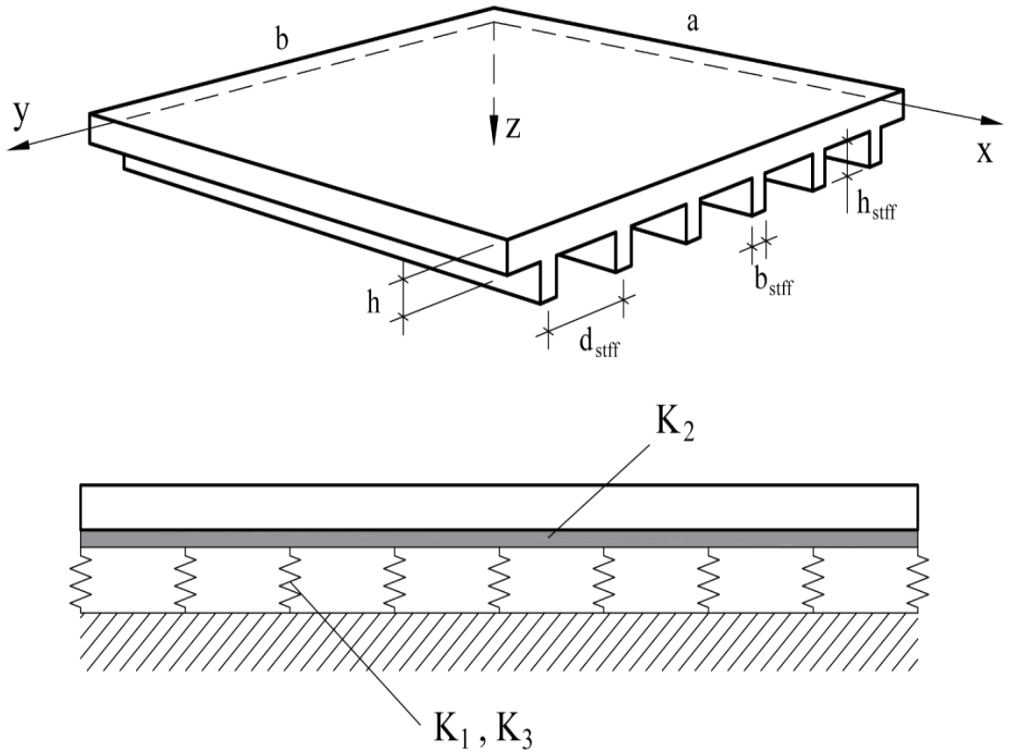

Fig. 4.1. Design of the stiffeners of the FG-CNTRC plates and geometric parameters of plates and stiffeners

4.2. Establishing the governing equations

HSDT is used taking into account the geometric imperfection of the plates with von Kármán geometric nonlinearity.

Expressions of internal forces N_i, moments M_i, and the higher-order moments T_i of the FG-CNTRC stiffened plates are expressed as

$$\begin{Bmatrix} N_x \\ N_y \\ N_{xy} \\ M_x \\ M_y \\ M_{xy} \\ T_x \\ T_y \\ T_{xy} \end{Bmatrix} = \begin{bmatrix} A_{11} & A_{12} & 0 & B_{11} & B_{12} & 0 & C_{11} & C_{12} & 0 \\ A_{12} & A_{22} & 0 & B_{12} & B_{22} & 0 & C_{12} & C_{22} & 0 \\ 0 & 0 & A_{66} & 0 & 0 & B_{66} & 0 & 0 & C_{66} \\ B_{11} & B_{12} & 0 & D_{11} & D_{12} & 0 & F_{11} & F_{12} & 0 \\ B_{12} & B_{22} & 0 & D_{12} & D_{22} & 0 & F_{12} & F_{22} & 0 \\ 0 & 0 & B_{66} & 0 & 0 & D_{66} & 0 & 0 & F_{66} \\ C_{11} & C_{12} & 0 & F_{11} & F_{12} & 0 & L_{11} & L_{12} & 0 \\ C_{12} & C_{22} & 0 & F_{12} & F_{22} & 0 & L_{12} & L_{22} & 0 \\ 0 & 0 & C_{66} & 0 & 0 & F_{66} & 0 & 0 & L_{66} \end{bmatrix}$$

$$\times \begin{Bmatrix} \varepsilon_x^0 \\ \varepsilon_y^0 \\ \gamma_{xy}^0 \\ \dfrac{\partial \phi_x}{\partial x} \\ \dfrac{\partial \phi_y}{\partial y} \\ \dfrac{\partial \phi_x}{\partial y} + \dfrac{\partial \phi_y}{\partial x} \\ -\lambda\left(\dfrac{\partial \phi_x}{\partial x} + \dfrac{\partial^2 w}{\partial x^2}\right) \\ -\lambda\left(\dfrac{\partial \phi_y}{\partial y} + \dfrac{\partial^2 w}{\partial y^2}\right) \\ -\lambda\left(\dfrac{\partial \phi_x}{\partial y} + \dfrac{\partial \phi_y}{\partial x} + 2\dfrac{\partial^2 w}{\partial x \partial y}\right) \end{Bmatrix} - \begin{Bmatrix} \varphi_{1x} \\ \varphi_{1y} \\ 0 \\ \varphi_{2x} \\ \varphi_{2y} \\ 0 \\ \varphi_{4x} \\ \varphi_{4y} \\ 0 \end{Bmatrix}, \tag{4.7}$$

where

$$\left(A_{ij},B_{ij},D_{ij},C_{ij},F_{ij},L_{ij}\right) = \left(A_{ij}^{P},B_{ij}^{P},D_{ij}^{P},C_{ij}^{P},F_{ij}^{P},L_{ij}^{P}\right)+\left(\bar{A}_{ij},\bar{B}_{ij},\bar{D}_{ij},\bar{C}_{ij},\bar{F}_{ij},\bar{L}_{ij}\right), \tag{4.8}$$

$$\left(A_{ij}^{P},B_{ij}^{P},D_{ij}^{P},C_{ij}^{P},F_{ij}^{P},L_{ij}^{P}\right)=\int_{-\frac{h}{2}}^{\frac{h}{2}} Q_{ij}^{P}(1,z,z^2,z^3,z^4,z^6)dz, \tag{4.9}$$

and

$$\begin{bmatrix}\bar{A}_{11} & \bar{B}_{11} & \bar{C}_{11}\\ \bar{B}_{11} & \bar{D}_{11} & \bar{E}_{11}\\ \bar{C}_{11} & \bar{E}_{11} & \bar{L}_{11}\end{bmatrix}=\begin{bmatrix}A_{11}^{stff} & B_{11}^{stff} & C_{11}^{stff}\\ B_{11}^{stff} & D_{11}^{stff} & F_{11}^{stff}\\ C_{11}^{stff} & F_{11}^{stff} & L_{11}^{stff}\end{bmatrix}$$

$$-\begin{bmatrix}A_{12}^{stff} & 0 & B_{12}^{stff} & 0 & C_{12}^{stff} & 0\\ B_{12}^{stff} & 0 & D_{12}^{stff} & 0 & F_{12}^{stff} & 0\\ C_{12}^{stff} & 0 & F_{12}^{stff} & 0 & L_{12}^{stff} & 0\end{bmatrix}\times$$

$$\begin{bmatrix}A_{22}^{stff} & 0 & B_{22}^{stff} & 0 & C_{22}^{stff} & 0\\ 0 & A_{66}^{stff} & B_{26}^{stff} & B_{66}^{stff} & 0 & C_{66}^{stff}\\ B_{22}^{stff} & 0 & D_{22}^{stff} & 0 & F_{22}^{stff} & 0\\ 0 & B_{66}^{stff} & 0 & D_{66}^{stff} & 0 & F_{66}^{stff}\\ C_{22}^{stff} & 0 & F_{22}^{stff} & 0 & C_{66}^{stff} & 0\\ 0 & L_{22}^{stff} & 0 & F_{66}^{stff} & 0 & L_{66}^{stff}\end{bmatrix}^{-1}\begin{bmatrix}A_{12}^{stff} & B_{12}^{stff} & C_{12}^{stff}\\ 0 & 0 & 0\\ B_{12}^{stff} & D_{12}^{stff} & F_{12}^{stff}\\ 0 & 0 & 0\\ C_{12}^{stff} & F_{12}^{stff} & L_{12}^{stff}\\ 0 & 0 & 0\end{bmatrix}, \tag{4.10}$$

and

$$\varphi_{1x}=\varphi_1^{xT}+\varphi_1^{x-stff}=\int_{-\frac{h}{2}}^{\frac{h}{2}}\left(Q_{11}^{P}\alpha_{11}^{P}+Q_{12}^{P}\alpha_{22}^{P}\right)\Delta T dz+\varphi_1^{x-stff},$$

$$\varphi_{1y}=\varphi_1^{yT}+\varphi_1^{y-stff}=\int_{-\frac{h}{2}}^{\frac{h}{2}}\left(Q_{12}^{P}\alpha_{11}^{P}+Q_{22}^{P}\alpha_{22}^{P}\right)\Delta T dz+\varphi_1^{y-stff}, \tag{4.11}$$

$$\left(A_{ij}^{stff},B_{ij}^{stff},D_{ij}^{stff},C_{ij}^{stff},F_{ij}^{stff},L_{ij}^{stff}\right)=$$

$$\frac{b_{stff}}{d_{stff}}\int_{\Omega}Q_{ij}^{stff}\left(1,z,z^2,z^3,z^4,z^6\right)dz,(i,j=1,2,6),$$

and $\varphi_1^{xS} = \dfrac{b_{stff}}{d_{stff}} \int_{\Omega} \left[Q_{11}^{stff} \alpha_{11}^{stff} + Q_{12}^{stff} \alpha_{22}^{stff} \right] \Delta T dz$, $\varphi_1^{y-stff} = 0$, for the case of plates stiffened by stiffeners in the direction x

$\varphi_1^{y-stff} = \dfrac{b_{stff}}{d_{stff}} \int_{\Omega} \left[Q_{11}^{stff} \alpha_{11}^{stff} + Q_{12}^{stff} \alpha_{22}^{stff} \right] \Delta T dz$, $\varphi_1^{x-stff} = 0$, for the case of the plates stiffened by stiffeners in the direction y.

The expressions for shear forces and higher-order shear forces are calculated as follows

$$\begin{Bmatrix} Q_x \\ Q_y \\ S_x \\ S_y \end{Bmatrix} = \begin{Bmatrix} H_{44} \dfrac{\partial w}{\partial x} + H_{44} \phi_x \\ H_{55} \dfrac{\partial w}{\partial y} + H_{55} \phi_y \\ H_{66} \dfrac{\partial w}{\partial x} + H_{66} \phi_x \\ H_{77} \dfrac{\partial w}{\partial y} + H_{77} \phi_y \end{Bmatrix}, \tag{4.12}$$

where

$$\begin{aligned} &\left(H_{44}, H_{55}, H_{66}, H_{77} \right) \\ &\quad = \left(H_{44}^P, H_{55}^P, H_{66}^P, H_{77}^P \right) + \left(\bar{H}_{44}, \bar{H}_{55}, \bar{H}_{66}, \bar{H}_{77} \right), \end{aligned} \tag{4.13}$$

and the plate is stiffened by stiffeners in the direction y of the plates

$$\begin{aligned} \bar{H}_{44} &= 0, \\ \bar{H}_{66} &= 0, \\ \bar{H}_{55} &= \frac{b_{stff}}{d_{stff}} \left(\int_{\Omega} Q_{44}^{stff} dz - 3\lambda \int_{\Omega} Q_{44}^{stff} z^2 dz \right), \\ \bar{H}_{77} &= \frac{b_{stff}}{d_{stff}} \left(\int_{\Omega} Q_{44}^{stff} z^2 dz - 3\lambda \int_{\Omega} Q_{44}^{stff} z^4 dz \right), \end{aligned} \tag{4.17}$$

with Ω is the integral region over the height of the stiffeners.

The equilibrium equation system of FG-CNTRC imperfect plate with stiffeners according to HSDT is written as follows [102]

$$\frac{\partial N_x}{\partial x}+\frac{\partial N_{xy}}{\partial y}=0,$$

$$\frac{\partial N_{xy}}{\partial x}+\frac{\partial N_y}{\partial y}=0,$$

$$\frac{\partial Q_x}{\partial x}+\frac{\partial Q_y}{\partial y}-3\lambda\left(\frac{\partial S_x}{\partial x}+\frac{\partial S_y}{\partial y}\right)+\lambda\left(\frac{\partial^2 T_x}{\partial x^2}+2\frac{\partial^2 T_{xy}}{\partial x\partial y}T_{xy,xy}+\frac{\partial^2 T_y}{\partial y^2}\right)$$

$$+N_x\left(\frac{\partial^2 w}{\partial x^2}+\frac{\partial^2 \bar{w}}{\partial x^2}\right)+2N_{xy}\left(\frac{\partial^2 w}{\partial x\partial y}+\frac{\partial^2 \bar{w}}{\partial x\partial y}\right)+N_y\left(\frac{\partial^2 w}{\partial y^2}+\frac{\partial^2 \bar{w}}{\partial y^2}\right)$$

$$+q-K_1 w+K_2\nabla^2 w-K_3 w^3=0,$$

$$\frac{\partial M_x}{\partial x}+\frac{\partial M_{xy}}{\partial y}+3\lambda S_x-\lambda\left(\frac{\partial T_x}{\partial x}+\frac{\partial T_{xy}}{\partial y}\right)-Q_x=0,$$

$$\frac{\partial M_{xy}}{\partial x}+\frac{\partial M_y}{\partial y}+3\lambda S_y-\lambda\left(\frac{\partial T_{xy}}{\partial x}+\frac{\partial T_y}{\partial y}\right)-Q_y=0, \qquad (4.18)$$

4.3. Boundary conditions and solution methods

Three simply supported boundary conditions are considered as follows:

- FG-CNTRC stiffened plates with four movable edges (FFFF)

- FG-CNTRC stiffened plates with two movable edges $x=0,\ x=a$ and the two remaining immovable edges $y=0,\ y=b$ (FIFI)

- FG-CNTRC stiffened plates with four immovable edges (IIII)

The solution forms of deflection, imperfection, and rotations are chosen in the following approximate forms [2, 7, 8, 102]

$$\begin{aligned} &w=W\sin\alpha x\sin\beta y,\quad \bar{w}=\xi h\sin\alpha x\sin\beta y,\\ &\phi_x=\Phi_x\cos\alpha x\sin\beta y,\quad \phi_y=\Phi_y\sin\alpha x\cos\beta y, \end{aligned} \qquad (4.27)$$

By substituting Eq. (4.27) into Eq. (4.23), after some calculations, the stress function can be obtained as

$$f=f_1\cos 2\alpha x+f_2\cos 2\beta y+f_3\sin\alpha x\sin\beta y+\frac{1}{2}N_{x0}y^2+\frac{1}{2}N_{y0}x^2, \qquad (4.28)$$

Substituting the relations (4.27) and (4.28) into Eqs. (4.24)-(4.26), and applying the Galerkin method, we get the equilibrium equations in the form of the nonlinear algebraic equation, as follows

$$
\begin{aligned}
&y_2 q+\left(y_1 N_{x0}+y_3 N_{y0}\right)\left(h\xi+W\right)+y_6\Phi_y+y_5\Phi_x\\
&+y_4\left(X_1\Phi_x+X_2\Phi_y\right)\left(h\xi+W\right)+y_7\left(2h\xi+W\right)W\left(h\xi+W\right)\\
&+y_8\left(2h\xi+W\right)W+y_4 X_3 W\left(h\xi+W\right)+y_9 W+y_{10}W^3=0,\\
&z_1\left(2h\xi+W\right)W+z_2 W+z_3\Phi_x+z_4\Phi_y=0,\\
&z_5\left(2h\xi+W\right)W+z_6 W+z_7\Phi_x+z_8\Phi_y=0,
\end{aligned}
\tag{4.29}
$$

4.4. Nonlinear buckling analysis

By extracting Φ_x and Φ_y from the last two of (4.29), and substituting into the first of (4.29), the load-deflection relation is obtained.

$$
\begin{aligned}
&y_{10}\left(\frac{W}{h}\right)^3 h^2+\left(\xi+\frac{W}{h}\right)\left(N_{x0}y_1+N_{y0}y_3\right)+u_8\frac{W}{h}+\frac{y_2 q}{h}\\
&+u_5\frac{W}{h}\left(\xi+\frac{W}{h}\right)h+u_6 h^2\left(2\xi+\frac{W}{h}\right)\frac{W}{h}\left(\xi+\frac{W}{h}\right)+u_7 h\left(2\xi+\frac{W}{h}\right)\frac{W}{h}=0,
\end{aligned}
\tag{4.30}
$$

For immovable edges, $u=0$ on both edges $x=0, x=a$ and $v=0$ on both edges $y=0, y=b$. The immovable conditions in the average sense are written as follows [2, 7, 8, 102]

$$
\int_0^b\int_0^a \frac{\partial u}{\partial x}dxdy=0, \tag{4.31}
$$

$$
\int_0^a\int_0^b \frac{\partial v}{\partial y}dydx=0. \tag{4.32}
$$

The expressions of N_{x0}, N_{y0} can be obtained form Eqs. (4.31) and (4.32), by using Eqs. (4.2), (4.7), (4.22) and (4.27), leading to

$$
N_{x0}=p_1\Phi_x+p_2\Phi_y+p_3 W\left(2h\xi+W\right)+p_4 W-\varphi_{1x}, \tag{4.33}
$$

$$
N_{y0}=p_5\Phi_x+p_6\Phi_y+p_7 W\left(2h\xi+W\right)+p_8 W-\varphi_{1y}, \tag{4.34}
$$

4.4.1. Buckling analysis of FG-CNTRC plates with FG-CNTRC stiffeners subjected only to external pressure

Substituting Eqs. (4.33) and (4.34) into Eq. (4.30), and applying $P_x=0$, the relation between q and W is obtained as

$$q = q_1 \frac{W}{h}\left(2\xi + \frac{W}{h}\right)\left(\xi + \frac{W}{h}\right) + q_2 \frac{W}{h}\left(2\xi + \frac{W}{h}\right) + q_3\left(\xi + \frac{W}{h}\right)\frac{W}{h}$$
$$+ q_4\left(\frac{W}{h}\right)^3 + q_5 \frac{W}{h} + h\left(\beta_1 \frac{a_1\varphi_{1x}}{a_2} + \beta_2 \frac{a_3\varphi_{1y}}{a_2}\right)\left(\xi + \frac{W}{h}\right), \quad (4.35)$$

4.4.2. Buckling analysis of FG-CNTRC plates with FG-CNTRC stiffeners subjected to external pressure and axial compression

In the case $q = 0$, the four edges are movable, coefficient $\beta_2 = 0$ is applied. Axial compression P_x is determined from Eq. (4.37)

$$P_x = \frac{1}{\left(\frac{W}{h} + \xi\right)(hy_1)}\left[\begin{array}{l} y_{10}\left(\frac{W}{h}\right)^3 h^2 + \frac{W}{h}\left(\frac{W}{h} + 2\xi\right)\left(\frac{W}{h} + \xi\right)e_5 \\ + e_6\left(\frac{W}{h} + 2\xi\right)\frac{W}{h} + e_8 \frac{W}{h}\left(\frac{W}{h} + \xi\right) + e_7 \frac{W}{h} \end{array}\right]. \quad (4.38)$$

Consider the second boundary condition, two edges $x = 0, a$ are movable, two edges $y = 0, b$ are immovable, $\beta_2 = 1$ is applied, obtained as

$$y_{10}\left(\frac{W}{h}\right)^3 h^2 + \frac{y_2 q}{h} + \left(2\xi + \frac{W}{h}\right)\frac{W}{h}\left(\xi + \frac{W}{h}\right)e_5$$
$$+ e_6\left(2\xi + \frac{W}{h}\right)\frac{W}{h} + e_8 \frac{W}{h}\left(\xi + \frac{W}{h}\right) + e_7 \frac{W}{h} \quad (4.40)$$
$$+ e_4\left(\xi + \frac{W}{h}\right)y_3\varphi_{1x} - \left(\xi + \frac{W}{h}\right)y_3\varphi_{1y} + \left(\xi + \frac{W}{h}\right)\left(y_3 z_1 - hy_1\right)P_x = 0.$$

4.6. Applying theoretical results to buckling analysis of FG-CNTRC plates with FG-CNTRC stiffeners

Table 4.2. Effect of CNT direction, stiffener, and thermal temperature on the critical axial compression P_x^{cr} of perfect FG-CNTRC plates (MPa, without elastic foundation, FFFF, UD)

ΔT(K)	X and Y plates without stiffeners	X plates and Y stiffeners	X plates and X stiffeners	Y plates and Y stiffeners	Y plates and X stiffeners
0	2.182	4,346	6,704	6,704	4,346
100	2.119	4.127	6,568	6,568	4.127
200	2,066	3,910	6,464	6,464	3,910

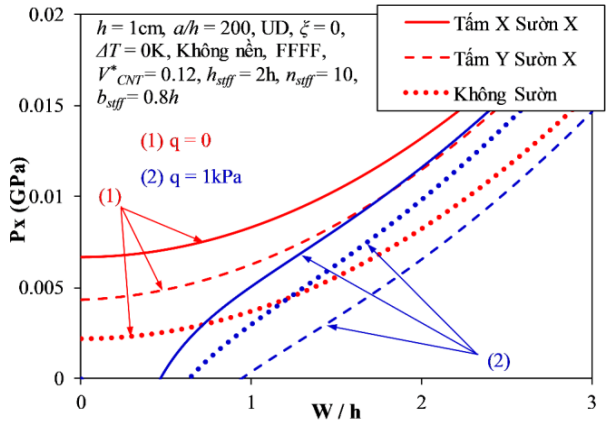

Fig. 4.3. Effect of stiffener direction on postbuckling behavior $P_x - W/h$ of FG-CNTRC plates

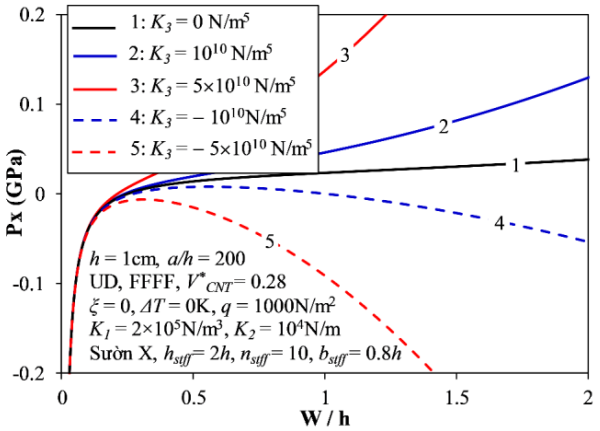

Fig. 4.14. Effect of nonlinear foundation stiffness on the postbuckling curve $P_x - W/h$ of stiffened plates

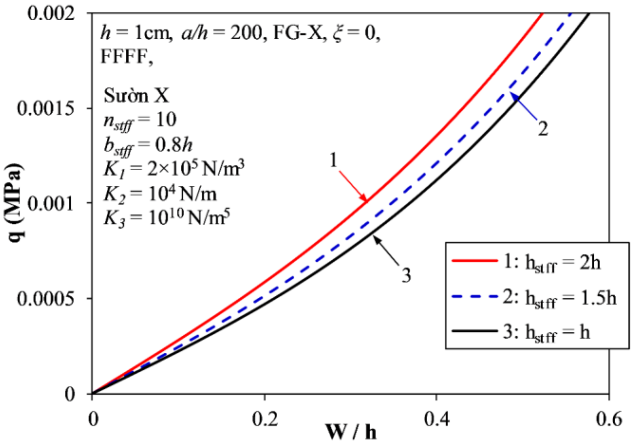

Fig. 4.15. Effect of stiffener height on the postbuckling curve $q - W/h$ of plates

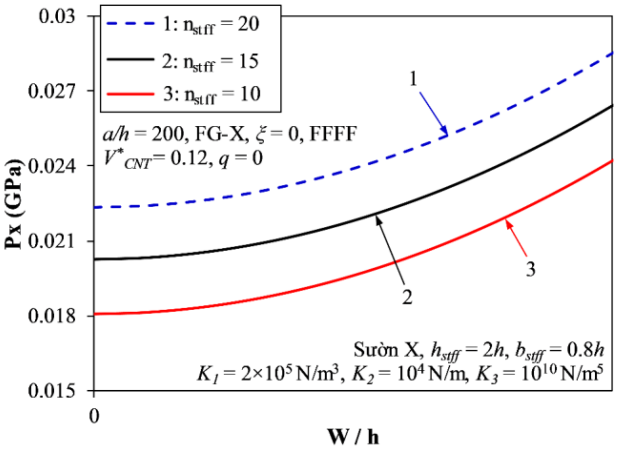

Fig. 4.18. Effect of stiffener number on the postbuckling curve $P_x - W/h$ of plates

4.7. Conclusion of Chapter 4

Numerical results show some notable points:

1. FG-CNTRC stiffeners significantly increase the critical axial compression and the postbuckling load capacity of the plates.

2. The effect of the FG-CNTRC stiffeners on the critical axial compression of the FG-V plates is the largest.

3. Nonlinear foundation stiffness does not affect the critical axial compression value of perfect plates.

4. Geometric parameters and thermal temperature significantly affect the critical axial compression and the postbuckling curve of the plates.

CONCLUSIONS

The thesis has obtained the following new results:

1. A method to stiffen FG-CNTRC cylindrical shells and plates with FG-CNTRC stiffeners, and CNT distribution rules for stiffeners suitable for FG-CNTRC cylindrical shells and plates are proposed. The improved smeared stiffener techniques for the FG-CNTRC stiffeners are developed. The stiffening solutions for the FG-CNTRC cylindrical shells with Auxetic core and CNT distribution rules for the coatings are proposed.

2. The governing equations of the nonlinear buckling problem of the FG-CNTRC cylindrical shells with stiffeners and Auxetic core in thermal environment are established. Three-term solutions are chosen to model the buckling and postbuckling behavior of two cases: cylindrical shell under external pressure and axial compression, and cylindrical shell under torsion.

3. The governing equations of the nonlinear buckling problem of the FG-CNTRC plates with stiffeners on the nonlinear elastic foundation are established. The solution form is chosen and the Galerkin method is applied to obtain buckling behavior expressions of the plates.

4 . Theoretical results are applied to analyze the effects of geometric parameters, and materials... on buckling and postbuckling behavior. The potential of applications in engineering and building design standards for FG-CNTRC plates and cylindrical shells in the future is shown.

RECOMMENDATIONS FOR FURTHER RESEARCH

1. Buckling and dynamic of FG-CNTRC plates and shells with stiffeners or Auxetic core under thermal and combined thermo-mechanical loads.
2. Nonlinear buckling and dynamic of FG-CNTRC structures with oblique FG-CNTRC stiffeners using FSDT and HSDT.
3. Buckling and dynamics of conical and truncated conical shells, spherical shell segment, FG-CNTRC revolution shell... considering stiffening method.
4. Buckling and dynamic of shells with complex shapes, discrete boundary conditions... made of FG-CNTRC considering the stiffening methods.
5. Research and develop the structural design standards for FG-CNTRC plates and shells for construction projects.

LIST OF THE AUTHOR'S SCIENTIFIC PUBLICATIONS RELATED TO THE THESIS

The thesis published 05 papers in ISI international journals (SCIE):

1. Dang Thuy Dong, Pham Thanh Hieu, Vu Minh Duc, Nguyen Thi Phuong, **Nguyen Van Tien**, Vu Hoai Nam. Nonlinear Buckling Analysis of Stiffened Carbon Nanotube-Reinforced Cylindrical Shells Subjected to External Pressure in Thermal Environment. Mechanics of Composite Materials 59, pp. 779–794 (2023).
2. Dang Thuy Dong, Vu Hoai Nam, Nguyen Thi Phuong, Le Ngoc Ly, Vu Minh Duc, **Nguyen Van Tien**, Tran Quang Minh, Vu Tho Hung, Pham Hong Quan. An analytical approach of nonlinear buckling behavior of longitudinally compressed carbon nanotube-reinforced (CNTR) cylindrical shells with CNTR stiffeners in thermal environment. ZAMM - Journal of Applied Mathematics and Mechanics 102, p. e202100228 (2022).
3. **Nguyen Van Tien**, Nguyen Thi Phuong, Vu Minh Duc, Tran Quang Minh, Dang Thuy Dong, Pham Hong Quan, Vu Hoai Nam, Le Ngoc Ly. Nonlinear Thermo-Mechanical Buckling of Torsion-Loaded Cylindrical Shells with Eccentric Stiffeners Made from CNT-Reinforced Composite. Iranian Journal of Science and Technology, Transactions of Mechanical Engineering 46, pp. 1107–1119 (2022).
4. Dang Thuy Dong, Nguyen Thi Phuong, Vu Hoai Nam, **Nguyen Van Tien**, Le Ngoc Ly, Vu Minh Duc, Tran Quang Minh, Vu Tho Hung, Nguyen Thi Huong Giang. An Analytical Approach for Nonlinear Buckling Analysis of Torsionally Loaded Sandwich Carbon Nanotube Reinforced Cylindrical Shells with Auxetic Core. Advances in Applied Mathematics and Mechanics 15 (2023), pp. 468-484.
5. Tran Quang Minh, Dang Thuy Dong, Vu Tho Hung, Cao Van Doan, **Nguyen Van Tien**, Pham Thanh Hieu. Geometrically Nonlinear Buckling of FG-CNTRC Plates Stiffened by FG-CNTRC Stiffeners Subjected to Combined Loads Using Nonlinear Reddy’s HSDT. International Journal of Structural Stability and Dynamics (2023). DOI: https://doi.org/10.1142/S0219455424501335